THE ASTROPHYSICAL JOURNAL, 325:853–863, 1988 February 15

MOLECULAR OUTFLOWS ASSOCIATED WITH BRIGHT FAR-INFRARED SOURCES

RONALD L. SNELL, Y.-L. HUANG, ROBERT L. DICKMAN, AND M. J. CLAUSSEN
Five College Radio Astronomy Observatory and Department of Physics and Astronomy, University of Massachusetts
Received 1987 June 22; accepted 1987 August 12

ABSTRACT

We have carried out a systematic search for high-velocity CO emission associated with bright 100 μm sources from the *IRAS* Point Source Catalog, in an effort to increase our understanding of the nature and evolutionary status of the objects producing molecular outflows. We selected 18 sources with 100 μm flux densities greater than 500 Jy and made maps in the $J = 1$–0 ^{12}CO line around each source. Almost every source observed was found to lie toward, or in the immediate vicinity of, strong CO emission and in most cases close to the maximum of this emission. Thus, all of the far-infrared sources can be associated with molecular clouds. Five of the sources show clear evidence of high-velocity molecular emission and at least three have bipolar morphologies. The newly detected outflow sources are all intrinsically luminous objects ($\sim 10^4$ $L_\odot$), and their outflows energetic ($\sim 10^{45}$ ergs). The infrared characteristics of all the sources in our survey suggest that they are young stellar objects still embedded in their parent molecular clouds. Statistics on the occurrence of outflows from bright far-infrared sources are used to set an upper limit of 4×10^5 yr for the dispersal time scale of material around young, luminous stellar objects.

Subject headings: infrared: sources — interstellar: molecules — stars: pre–main-sequence

I. INTRODUCTION

Young stellar objects are frequently associated with energetic outflows of molecular gas. As a result of extensive searches made during the past 5 years, more than 70 such outflows are presently known (Lada 1985; Snell 1987). However, these searches were neither systematic nor statistically complete, owing primarily to the lack of a good census of young stellar objects in molecular clouds. Thus the frequency of the outflow phenomenon and the nature and evolutionary status of the objects responsible for it remain unclear. While past outflow surveys have largely relied on optical catalogs of sources (Edwards and Snell 1985; Levreault 1985), more systematic outflow searches are now possible using the wealth of data provided by the *Infrared Astronomical Satellite* (*IRAS*). Several such surveys have been completed and have been successful in detecting outflows from regions of low-mass star formation (Heyer *et al.* 1987; Myers *et al.* 1987) and in identifying good outflow candidates from a sample of unidentified *IRAS* sources of low color temperature (Casoli *et al.* 1986).

We have taken advantage of the *IRAS* Point Source Catalog (1985) to survey a complete sample of bright far-infrared (FIR) sources for high-velocity molecular emission. We have chosen sources based solely on their infrared properties and have made maps around each to determine if outflows are present. Thus, unlike many past surveys which were biased toward sources known to have unusually broad CO emission or in which outflow detections were based on a single spectrum, our survey avoids such a bias and has sufficiently large maps to confirm the outflow nature of sources found. Our selection criteria were the following: (1) the sources were required to have $S(100\ \mu\text{m}) > 500$ Jy, (2) their right ascension had to lie between R.A. = 0^h and 12^h, and (3) their declination had to be greater than 0°. The latter criteria were imposed both to avoid lines of sight through the inner Galaxy where it is difficult to separate the complicated galactic emission from high-velocity outflows, and to ensure that the sources transited at reasonably high elevations at the Five College Radio Astronomy Observatory (FCRAO). Finally, to ensure that our sample consisted of decisively stellar objects, we required the sources to be detected at all four *IRAS* bands and to have also been detected in the earlier Air Force Geophysics Laboratory (AFGL) surveys (Price and Walker 1976; Price 1977). Excluding IRC +10216 and M82, 26 *IRAS* sources met all of the above criteria and eight were already well-studied sources that were known to have associated outflows (Lada 1985). The remaining 18 bright 100 μm sources were mapped in ^{12}CO emission and the resulting spectra analyzed for high-velocity molecular gas. The results of this survey are presented in § II and a detailed discussion of the five outflows discovered is presented in § III. Finally, the statistics on outflow occurrence and energetics of the newly discovered outflows are presented in § IV.

II. OBSERVATIONS AND RESULTS

The observations of the $J = 1$–0 transition of ^{12}CO were made with the 14 m telescope of the Five College Radio Astronomy Observatory in New Salem, Massachusetts. At a frequency of 115 GHz, the FCRAO telescope has a beamwidth of 45″ and a forward spillover and scattering efficiency of 0.70. These values have been established from observations of the Moon and planets. All temperatures in this paper are in units of T_R^*, i.e., antenna temperature corrected for atmospheric, spillover, and scattering losses from the antenna and radome (Kutner and Ulich 1981). An additional correction would be needed to account for the source coupling efficiency; we estimate this additional correction to be ~ 0.7 for the sources mapped, since they are rather small in angular extent.

We began our survey by first obtaining a map of 3×3 points, spaced by 1′.5 and centered on each of the 18 *IRAS* point sources. This search strategy was adopted to reduce the chances that high-velocity emission would be missed, since such emission is often extended and distinctly separated from the driving source (Snell, Loren, and Plambeck 1980; Goldsmith *et al.* 1984). The positions of the 18 *IRAS* point sources observed are given in Table 1. In most sources, follow-up mapping was done to better define the nature and extent of the molecular emission.

TABLE 1

SUMMARY OF CO OBSERVATIONS

AFGL	*IRAS*	R.A.(1950)	Decl.(1950)	T_R^* (K)	V_{LSR} (km s^{-1})	V	Secondary V (km s^{-1})
328	02230+6202	02^{h}23^{m}02^s.3	+62°02′24″	9.1	−43.0	3.8	−39, −33
4029	02575+6017	02 57 35.6	+60 17 22	23.8	−38.9	5.5	...
416	02593+6016	02 59 20.6	+60 16 08	9.6	−38.5	3.2	...
5090	03064+5638	03 06 26.9	+56 38 56	8.6	−39.8	2.4	...
5094	03211+5446	03 21 11.8	+54 46 51	5.0	−31.3	1.9	−25, −12, +3
5124	04324+5106	04 32 28.7	+51 06 39	9.1	−35.6	5.7	−6, −1, +4
5137	05100+3723	05 10 01.7	+37 23 35	11.7	−6.4	4.0	...
5142	05274+3345	05 27 27.6	+33 45 37	12.6	−4.1	5.5	...
5144	05281+3412	05 28 07.8	+34 12 46	3.8	−4.8	2.2	...
5157	05345+3157	05 34 32.6	+31 57 40	9.9	−17.7	5.2	...
5158	05355+3039	05 35 34.0	+30 39 48	5.7	−15.8	4.1	+1
6366S.....	06056+2131	06 05 40.9	+21 31 32	16.4	+2.8	5.3	...
5180.....	06058+2138	06 05 53.9	+21 38 57	17.0	+4.2	6.7	...
5182	06061+2151	06 06 07.3	+21 51 12	10.8	−1.6	4.5	...
5183.....	06063+2040	06 06 23.0	+20 40 02	7.0	+8.9	5.1	+4
5184	06068+2030	06 06 53.0	+20 30 41	18.8	+8.9	2.8	...
5185	06073+1249	06 07 23.5	+12 49 24	16.2	+25.1	2.7	...
5188	06114+1745	06 11 28.6	+17 45 33	10.1	+8.2	5.3	...

CO emission was detected toward all 18 *IRAS* point sources and a summary of the emission seen toward each source is compiled in Table 1. In 13 sources only a single velocity component was detected and in five sources, two or more velocity components were found. In these latter five sources, one of the components was always considerably stronger than the rest, and it is this feature's intensity that is given in Table 1. The velocities of any secondary emission components are also given in Table 1. The emission seen toward most sources is very strong, exceeding 9 K in 13 of the 18 sources. This suggests that the *IRAS* sources are intimately associated with the molecular clouds producing the CO features and play a role in heating the surrounding molecular material. Maps of peak CO emission intensity are shown in Figure 1 for 12 of the sources, and maps of integrated intensity are shown in Figure 2 for the other six sources. As can be seen in these maps, the maximum CO emission is found very close to the location of the *IRAS* source in all cases but AFGL 328, AFGL 5094, and AFGL 5183. In the latter two sources the location of the peak CO emission is not well defined but is significantly displaced from the position of the *IRAS* source. AFGL 328 is the only region in which the small map that we made does not clearly identify a maximum in the CO emission; a larger scale map of the W3N region made by Thronson *et al.* (1984) and Huang and Thaddeus (1986) shows that the far-infrared source is located in the center of an extended molecular cloud. Thus, in most sources there is good reason to believe that the velocity component identified in Table 1 is indeed emission from molecular gas associated with the FIR source.

Most of the infrared sources in our sample have Galactic coordinates and velocities (based on the associated CO emission) that would place them in the Perseus arm (Roberts 1972). Because the Perseus arm is known to have systematic streaming motions relative to normal galactic rotation (Roberts 1972), kinematic distances based on models of the galaxy with only circular motion are not reliable. In addition, many of our sources lie very near the anticenter direction, where kinematic distances cannot be determined. To estimate the distance to each source, we have therefore used known distances to H II regions and OB associations that lie near the far-infrared sources and which have similar velocities. Several of our infrared sources coincide with exciting stars of H II regions that have reliably determined distances. Other infrared sources lie near H II regions or OB associations and their distances are based on their assumed association with these objects. Thus, distances to these latter sources are less reliable. The least reliable distances are for those infrared sources where we had no option but to use the kinematic distance. A summary of our distance estimates is presented in Table 2. We have used the FIR flux densities from the *IRAS* Point Source Catalog (1985) and the distances tabulated in Table 2 to estimate FIR luminosities for our sources, employing the expression for the total FIR flux given by Casoli *et al.* (1986) and using the flux densities at all four *IRAS* wavelength bands.

TABLE 2

DISTANCES AND LUMINOSITIES OF SOURCES

Source	Distance (kpc)	Reference	FIR Luminosity ($L_\odot$)
AFGL 328 (W3N)	2.2	1	5.3×10^4
AFGL 4029 (IC 1848)	2.2	1	2.1×10^4
AFGL 416 (S201)	2.2	1	2.6×10^4
AFGL 5090	4.1	2	2.9×10^4
AFGL 5094	3.1	2	2.4×10^4
AFGL 5124	6.0	3	1.1×10^5
AFGL 5137 (S228)	2.6	4	1.4×10^4
AFGL 5142	1.8	5	8.1×10^3
AFGL 5144 (S237)	1.8	6	1.1×10^4
AFGL 5157	1.8	7	5.5×10^3
AFGL 5158	1.8	7	4.5×10^3
AFGL 6366S	1.5	8	2.0×10^4
AFGL 5180	1.5	8	1.1×10^4
AFGL 5182	1.5	8	1.0×10^4
AFGL 5183	1.5	8	1.2×10^4
AFGL 5184 (S252)	1.5	9	7.7×10^3
AFGL 5185	4.8	10	4.8×10^4
AFGL 5188	2.5	11	1.6×10^4

REFERENCES.—(1) Associated with Cas OB6 (Humphreys 1978); (2) kinematic distance; (3) near S212 (Moffett, FitzGerald, and Jackson 1979; MFJ); (4) S228 kinematic distance (Georgelin, Georgelin, and Roux 1973); (5) near S237 (MFJ 1979); (6) coincident with S237 (MFJ 1979); (7) near S235 (Evans and Blair 1981); (8) associated with Gem OB1 (Humphreys 1978); (9) coincident with S252 (MFJ 1979); (10) near S271 and S272 (MFJ 1979); (11) near S255 (MFJ 1979).

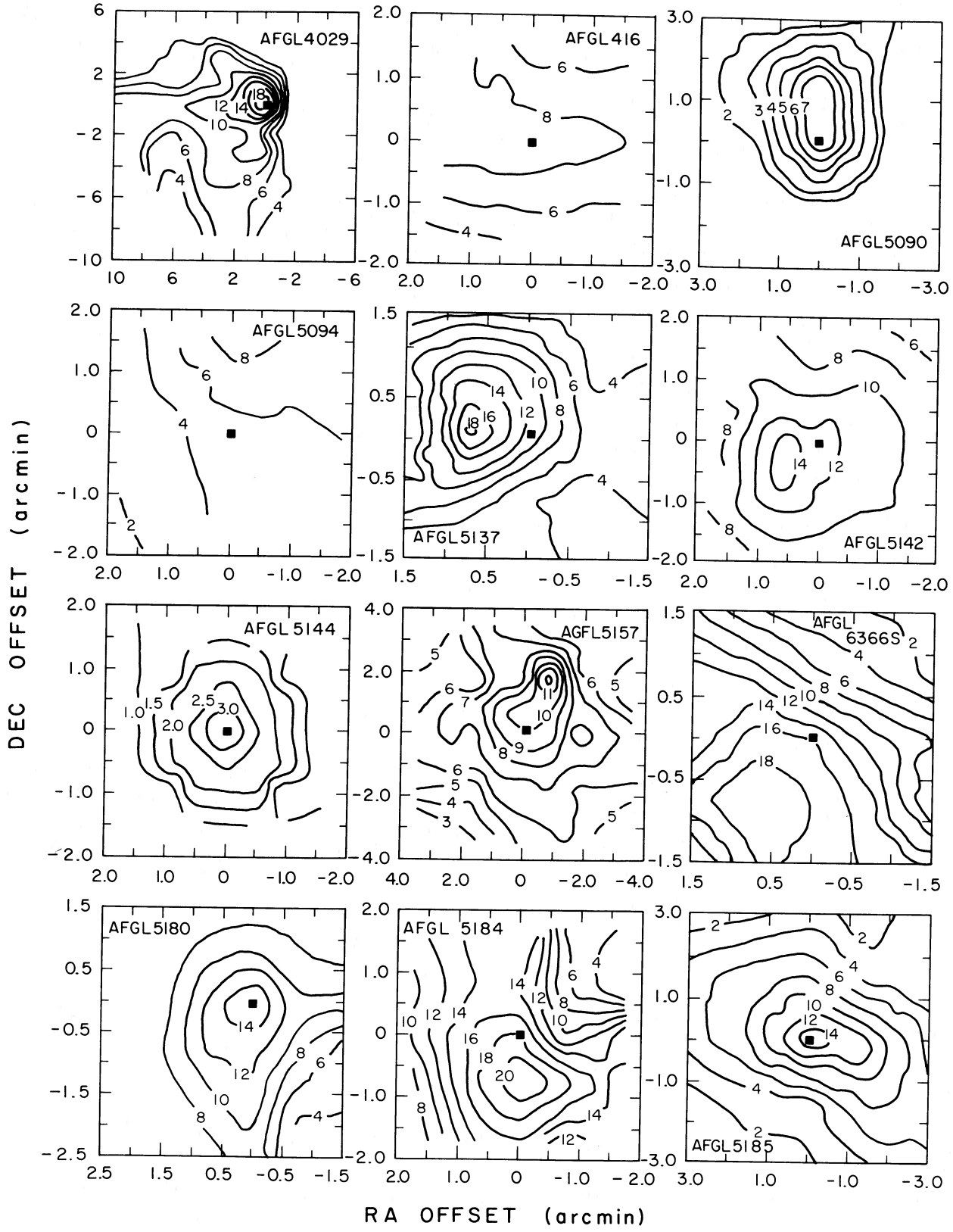

FIG. 1.—Maps of the peak ^{12}CO antenna temperature (T_R^*) around 12 of the far-infrared sources in our survey. The location of the far-infrared sources are marked by filled squares; in most cases these sources lie near the peak in the CO emission.

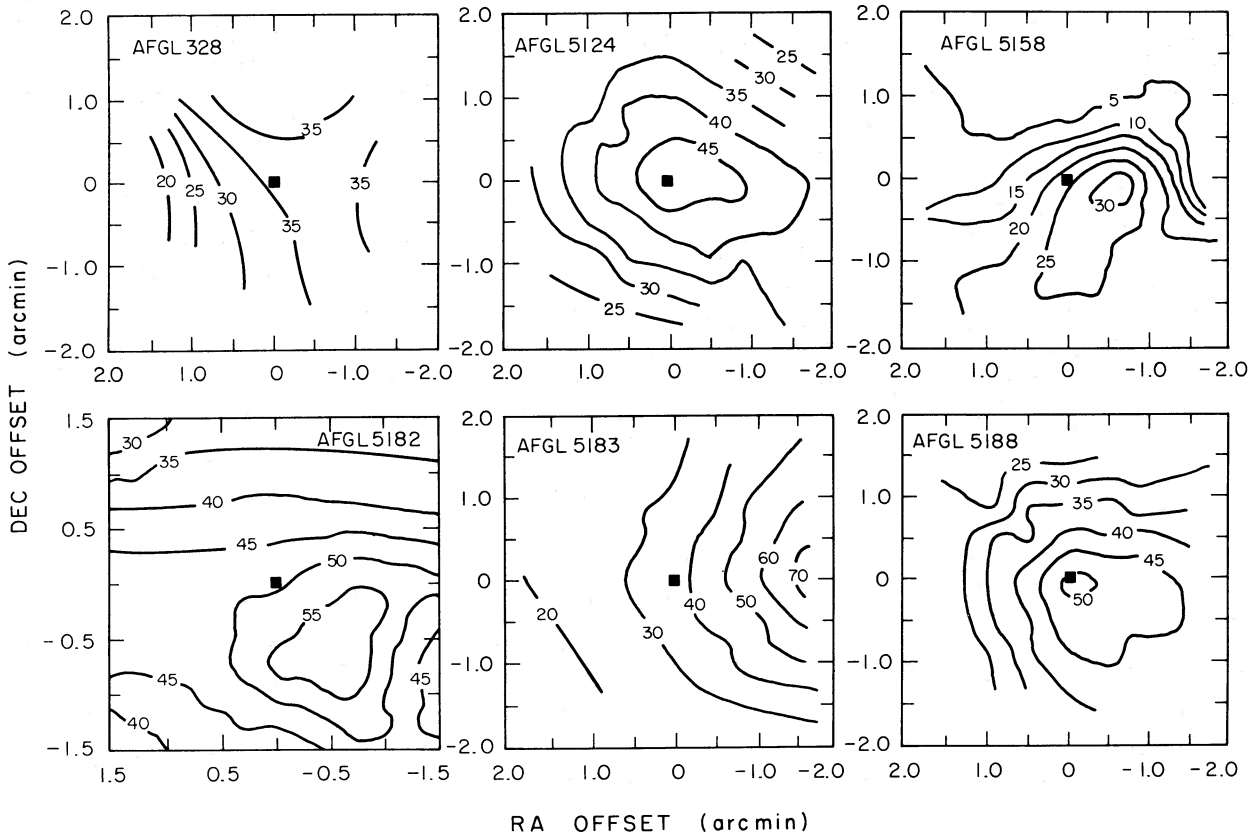

FIG. 2.—Maps of the integrated ^{12}CO antenna temperature around six of the far-infrared sources in our survey. The location of the far-infrared sources are marked by filled squares; in most cases these sources lie near the peak in the integrated CO emission.

Estimates of the FIR luminosities are given in Table 2 and vary between 4.5×10^3 and 1.1×10^5 $L_\odot$, a surprisingly narrow range of values. Thus, all of the objects in our sample are intrinsically luminous. In addition, the far-infrared colors of the sources are also very similar, with average flux-density ratios of [100 μm/60 μm] = 1.55 ± 0.37, [60 μm/25 μm] = 9.4 ± 4.6, and [25 μm/12 μm] = 5.8 ± 3.4. Thus, the sources surveyed are all extremely red and lie in the same region of the color-color diagram where one finds young, embedded, stellar objects (Emerson 1987). Hence, as suggested by their coincidence with strong molecular emission, all of our sources are probably young O and B stars embedded in molecular clouds associated with the Perseus spiral arm.

III. MOLECULAR OUTFLOWS

Based on our initial nine-point maps, we searched for evidence of outflow activity. The first criterion used in selecting sources for further observations was the existence of a large velocity extent. Snell (1987) found in single-velocity component molecular clouds that total velocity extents greater than 10 km s^{-1} usually indicated the presence of an outflow. Thus, in all sources with velocity extents greater than 5 km s^{-1}, we extended the ^{12}CO maps. However, large velocity extent alone does not necessarily imply the presence of an outflow; and one must be careful to recognize the presence of additional velocity components that could mimic high-velocity motion. Therefore, we also required that high-velocity wings be spatially restricted to the vicinity of the FIR source. Sufficiently large maps were made to ensure that this was the case. A brief description of each of the five new outflows that were found is presented in the following subsections.

a) AFGL 4029

AFGL 4029 lies near the H II region IC 1848 and has the strongest CO emission of any source in the survey. Our distance estimate of 2.2 kpc is based on a presumed association with the Cas OB6 association (Humphreys 1978) and is consistent with the distance estimated for the exciting star HD 18326 (Georgelin and Georgelin 1976) of IC 1848. The IC 1848 region has been extensively studied by Loren and Wootten (1978) and Wootten *et al.* (1983) and the infrared source lies toward the bright rim IC 1848A. The CO emission (See Fig. 1) is strongly peaked in the direction of the FIR source and the broad wings seen toward this source were first noted by Wootten *et al.* (1983). A spectrum obtained toward AFGL 4029 is presented in Figure 3 which shows high-velocity wings having a total velocity extent of 15 km s^{-1}. Away from AFGL 4029, emission in the velocity intervals -36 to -30 km s^{-1} (red) and -46 to -40 km s^{-1} (blue) disappears. A contour map of the integrated emission in the red and blue wings is shown in Figure 4. The peak emission in both the red and blue wings is coincident with AFGL 4029 and is distributed symmetrically about this source. The outflow has a radius of ~ 0.6 pc and is restricted to a small portion of the IC 1848A molecular cloud.

b) AFGL 5142

AFGL 5142 is probably part of a large star-formation complex that includes a number of H II regions (S231–S237;

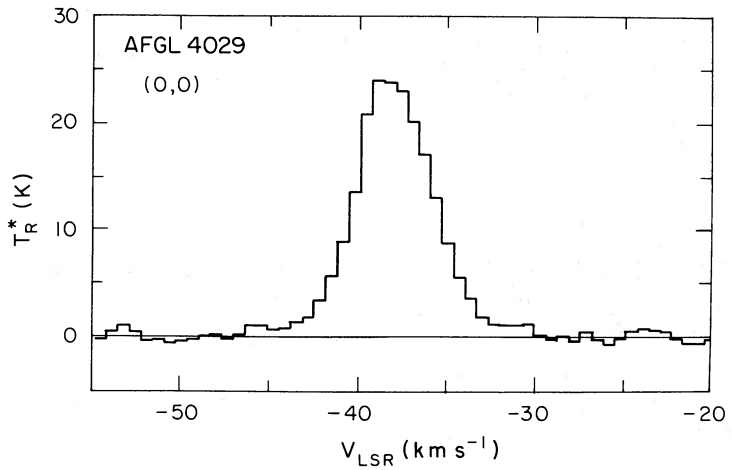

FIG. 3.—Spectrum of the ^{12}CO line toward AFGL 4029

Sharpless 1959). The velocity of the CO emission detected toward these H II regions (Blitz, Fich, and Stark 1985) is identical to that found for the CO emission associated with AFGL 5142. In angular offset, the closest of the H II regions is S237, which lies within 0°.5 of AFGL 5142. Based on the similarity in position and velocity to S237, we have assumed that AFGL 5142 is at the same distance of 1.8 kpc estimated for S237 (Moffat, FitzGerald, and Jackson 1979). Spectra obtained 0°.75 east and west of AFGL 5142 are shown in Figure 5 and illustrate the weak wings present in this region. The blue wing is more prominent west of the source and the red wing is more prominent east of the source. The total velocity extent is 12 km s^{-1}, the smallest of the five outflows detected. A contour map of the integrated emission in the blue wing (−12 to −6 km s^{-1}) and the red wing (−1 to 5 km s^{-1}) is shown in Figure 6. This map shows quite clearly the asymmetrical distribution of the red and blue wings about AFGL 5142, a pattern characteristic of bipolar outflows. Again, as in AFGL 4029, the high-velocity emission has a small spatial extent and is centered on the far-infrared source. The radius of the outflow is 0.6 pc at a distance of 1.8 kpc.

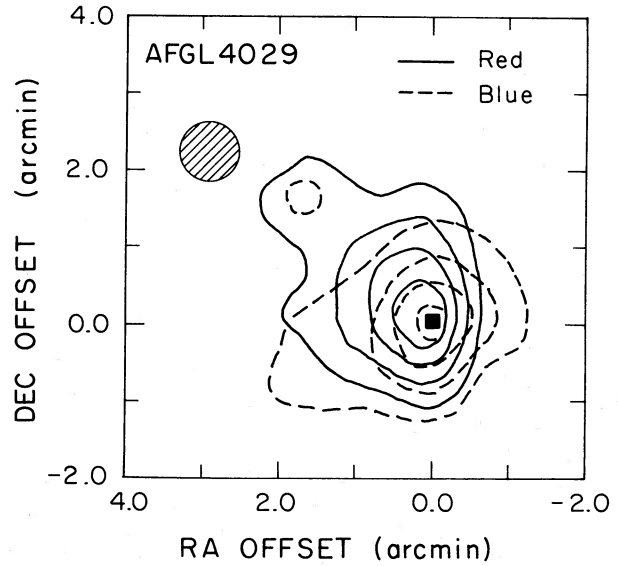

FIG. 4.—Maps of the integrated ^{12}CO intensity of the high-velocity red shifted (−36 to −30 km s^{-1}) and blueshifted (−46 to −40 km s^{-1}) emission near AFGL 4029. The location of AFGL 4029 is indicated by the filled square and the full width at half-power (FWHP) beam size is indicated by the cross-hatched circle

c) *AFGL 5157*

AFGL 5157 lies several degrees southeast of the AFGL 5142 and is probably also part of the star-forming complex in which S231–S237 are contained. The velocity of the CO emission from AFGL 5157 is similar to both S235 and S237, which lie several degrees farther to the southeast. We have therefore assumed for this object the distance of 1.8 kpc found for the H II regions S235 and S237 (Evans and Blair 1981; Moffat, FitzGerald, and Jackson 1979). Three spectra obtained in the vicinity of AFGL 5157 are shown in Figure 7 and reveal striking, high-velocity wings. The total velocity extent is 23 km s^{-1}, the largest of the five outflows found. A contour map of integrated intensity in the blue wing (−30 to −22 km s^{-1}) and red wing (−15 to −5 km s^{-1}) is presented in Figure 8. This map shows clearly the bipolar nature of the outflow, but the center of the outflow is located 0°.75 north and 0°.75 east of AFGL 5157. Searches for additional far-infrared sources (*IRAS Point Source Catalog*, 1985) reveal no better candidates for the origin of the molecular outflow. This offset could be real, resulting from a complex flow pattern of the winds from this source, or alternatively, could be due to an error in the position of AFGL 5157 as determined by the *IRAS* satellite. Further analysis of the *IRAS* data or further infrared observations may be necessary to determine the location of this infrared source accurately.

d) *AFGL 6366S*

AFGL 6366S is located in a complex of molecular clouds (Huang and Thaddeus 1986) associated with a number of H II regions including S247, S249, S252, and S254–S258. Distance estimates for these H II regions vary from 1.5 kpc for S252 (Humphreys 1978) to 3.5 kpc for S247 (Moffat, FitzGerald, and Jackson 1979). AFGL 6366S lies closest to S247 and its CO emission is at the same velocity as the CO emission seen toward S247 (Blitz, Fich, and Stark 1982). Thus, it would appear reasonable to assign a distance to AFGL 6366S of 3.5 kpc, the distance found for S247. Unfortunately, the distance

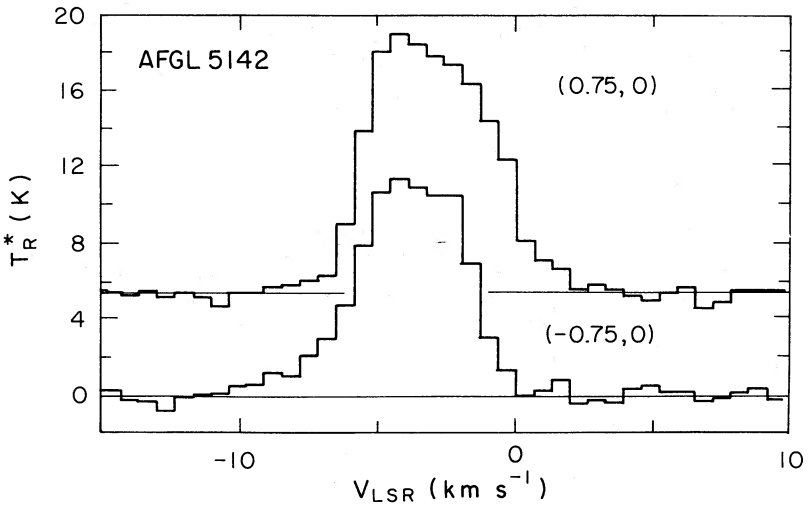

FIG. 5.—^{12}CO spectra obtained 0.75 east and west of AFGL 5142

determination for S247 is based on only one star and the velocity of the H II region is 4.5 km s^{-1} higher than that found for the CO emission detected toward AFGL 6366S (Georgelin, Georgelin, and Roux 1973). The molecular clouds associated with S252 and S254–S258 have been studied by Lada and Wooden (1979) and Evans, Blair, and Beckwith (1979) and the velocity of the CO emission is roughly 7.5 km s^{-1}, more than 4 km s^{-1} higher than the velocity found for the CO emission associated with AFGL 6366S, but similar to the 7.4 km s^{-1} found for S247. Thus, it is not clear with which region to associate AFGL 6366S. The source lies in the general direction of the Gem OB1 association and an extensive study of the OB stars in this association indicate a distance of 1.5 kpc (Humphreys 1978). Because of the confusion and potential uncertainties in the distances to individual H II regions, we have adopted the distance of 1.5 kpc to the Gem OB1 association for AFGL 6366S.

Two CO spectra obtained in the vicinity of AFGL 6366S are shown in Figure 9. These spectra show the striking wings associated with this object and also that the red and blue wings are not spatially coincident. The total velocity extent for this outflow is 18 km s^{-1}. A contour map of the integrated intensity in the red wing (6 to 14 km s^{-1}) and blue wing (-10 to -2 km s^{-1}) is presented in Figure 10. The map shows quite clearly the bipolar nature of this outflow, but as in AFGL 5157, the far-infrared source is not found midway between the strong emission in the red and blue wings. No other far-infrared sources are known to be present in this region; thus, as in AFGL 5157, either the position of the far-infrared sources is in error, or the large-scale outflow is not symmetrically centered about the driving stellar source.

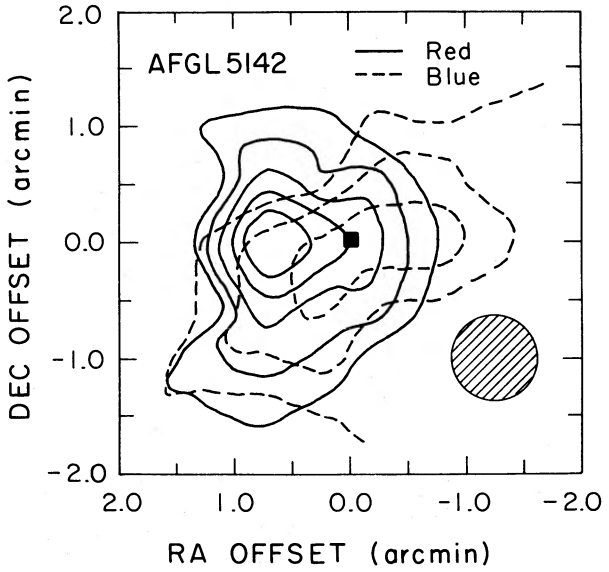

FIG. 6.—Maps of the integrated ^{12}CO intensity of the high-velocity redshifted (-1 to 5 km s^{-1}) and blueshifted (-12 to -6 km s^{-1}) emission near AFGL 5142. The location of AFGL 5142 is indicated by the filled square and the FWHP beamsize is indicated by the cross-hatched circle.

e) AFGL 5180

AFGL 5180 lies within 10′ of AFGL 6366S, and the CO emission associated with AFGL 5180 is at nearly the same velocity as that associated with AFGL 6366S. The two FIR sources are thus almost certainly associated with each other. We will assume a distance to AFGL 5180 of 1.5 kpc, the same distance assumed for AFGL 6366S. A CO spectrum obtained toward the FIR source is shown in Figure 11 and has a full velocity width of 15 km s^{-1}, indicating the presence of an outflow. Attempts to map the extent of the red and blue wings are hampered by the presence of a secondary velocity component at 8 km s^{-1} that is found away from the position of the FIR source (see the bottom spectrum in Fig. 11). The additional component occurs at the velocity of the emission associated with S252–258 and probably represents the projected overlap of the molecular clouds associated with these H II regions and the molecular cloud associated with AFGL 5180. Unfortunately, the presence of this component makes it impossible to trace the extent of the redshifted emission associated with the outflow; in fact, the red wing seen toward the infrared source may also be due to this overlapping molecular cloud. The blue wing does not appear to be contaminated, and a map of the integrated intensity from -8 to 0 km s^{-1} is shown in Figure 12. The blueshifted emission is roughly centered on the

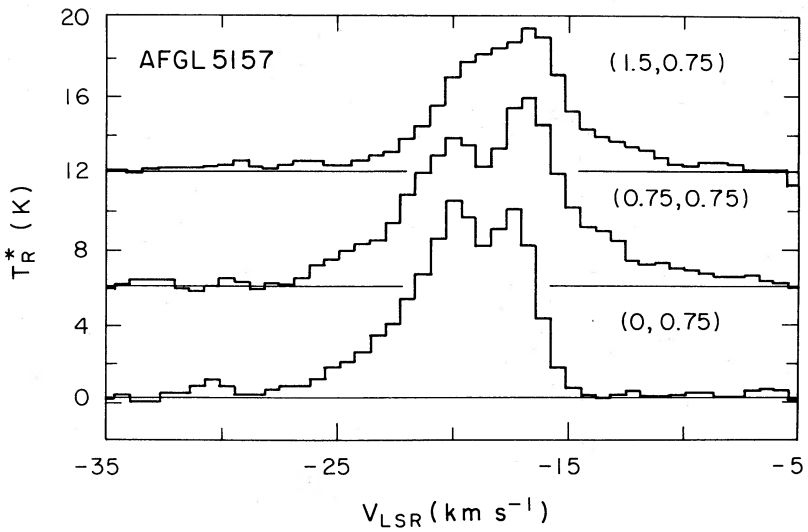

FIG. 7.—^{12}CO spectra obtained in three locations near AFGL 5157. The positions where these spectra were obtained is given as an offset in arcminutes relative to AFGL 5157.

source but little can be determined concerning the geometry of this outflow.

IV. DISCUSSION

Our observations have identified molecular clouds associated with all 18 FIR sources in our survey. This association, coupled with the *IRAS* colors of these sources, suggests that they are all young stellar objects with bolometric luminosities ranging from 4×10^3 to 1.1×10^5 $L_\odot$. Thus, they are presumably young O and B stars, most of which are located in the Perseus arm (Roberts 1972). Of the 18 sources surveyed, five were found to have high-velocity wings, constituting evidence for molecular outflows. Detailed maps of the CO emission from these five objects showed that three have a bipolar geometry, one shows no sign of a bipolar nature, and the last has confusing emission that precludes a determination of the geometry of the outflow. In the following sections we estimate the energetics of the five newly discovered outflows and discuss the frequency and importance of such outflows in the evolution of massive star-forming molecular clouds.

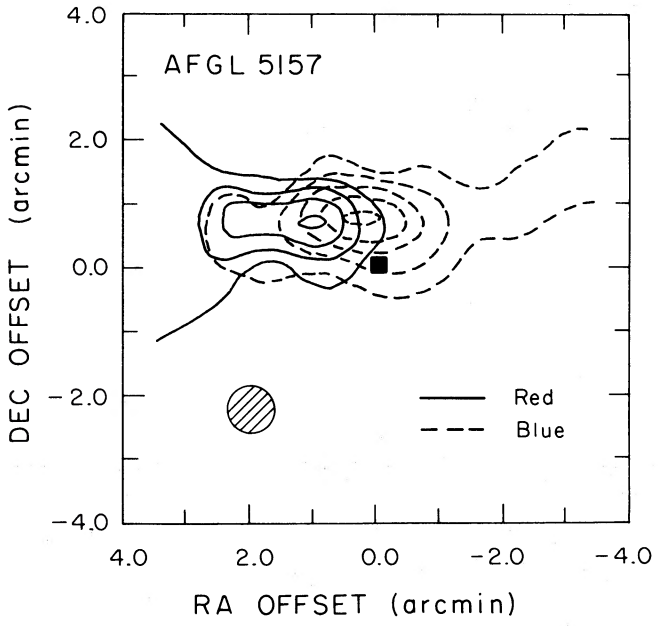

FIG. 8.—Maps of the integrated ^{12}CO intensity of the high-velocity redshifted (-15 to -5 km s^{-1}) and blueshifted (-30 to -22 km s^{-1}) emission near AFGL 5157. The location of AFGL 5157 is indicated by the filled square and the FWHP beamsize is indicated by the cross-hatched circle.

a) Energetics of the Molecular Outflows

We have estimated the mass, momentum, and energy of the outflowing molecular gas using techniques similar to those employed by Snell *et al.* (1984). To determine the column density of high-velocity gas, we have assumed that the CO emission is optically thin and that the populations of the various rotational levels are in LTE and are thus specified by the gas temperature. The ambient cloud temperature based on the CO emission is found to be between 10 and 20 K, but the dust temperature based on the ratio of 60 to 100 μm flux density is considerably higher. For an emissivity that is inversely proportional to the wavelength, the average dust temperature is 40 K. We have adopted a gas temperature for the outflows of 25 K for our calculations of the outflow column density. Thus, the CO column density is given by: $N(\mathrm{CO}) = 1.4 \times 10^{15} \int T_R\, dv\ \mathrm{cm}^{-2}$, where the integration is carried out over the line profile. To estimate the total gas column density, we have assumed a CO/H_2 ratio of 10^{-4}. Snell *et al.* (1984) found that the optical depth of the high-velocity CO emission was greater than unity at some velocities and used the measured ^{13}CO intensity to correct the "optically thin" column densities for the optical depth effects. Unfortunately, we do not have ^{13}CO observations of the outflows under study, and therefore the column densities that we determine are lower limits to the true column densities of high-velocity gas.

The mass of outflowing molecular gas can now be estimated by summing up the computed column densities of high-velocity gas over the extent of the map. The masses of high-

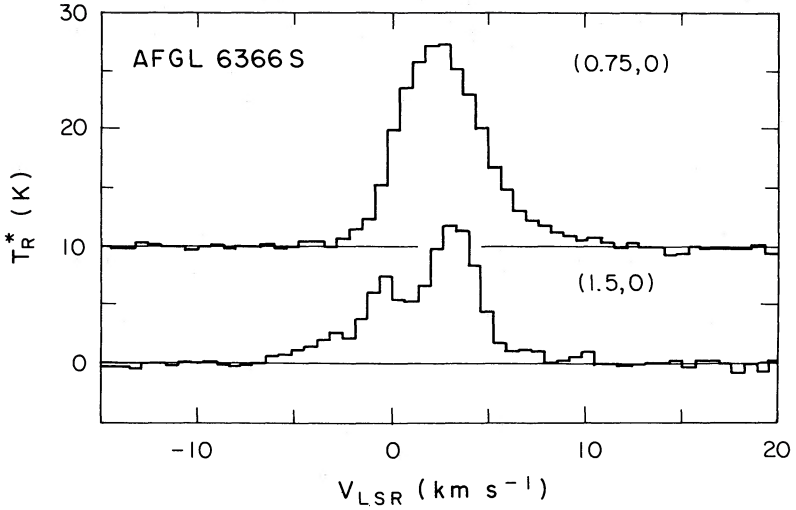

FIG. 9.—^{12}CO spectra obtained 0.'75 and 1'.5 east of AFGL 6366S

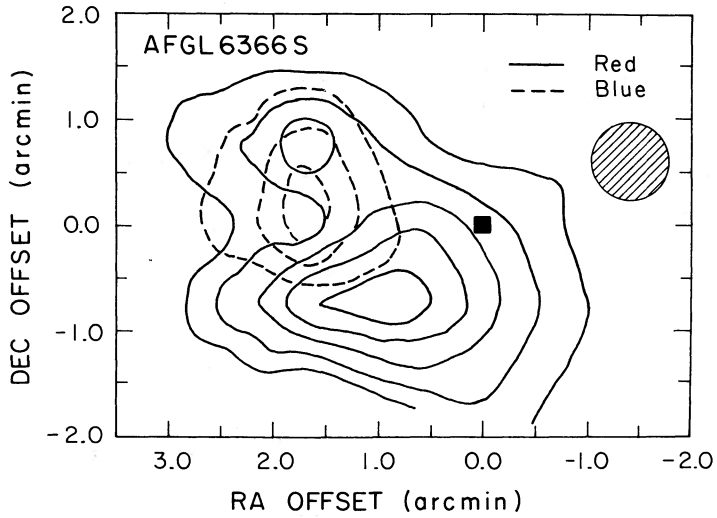

FIG. 10.—Maps of the integrated ^{12}CO intensity of the high-velocity redshifted (6 to 14 km s^{-1}) and blueshifted (-10 to -2 km s^{-1}) emission near AFGL 6366S. The location of AFGL 6366S is indicated by a filled square and the FWHP beam size is indicated by the cross-hatched circle.

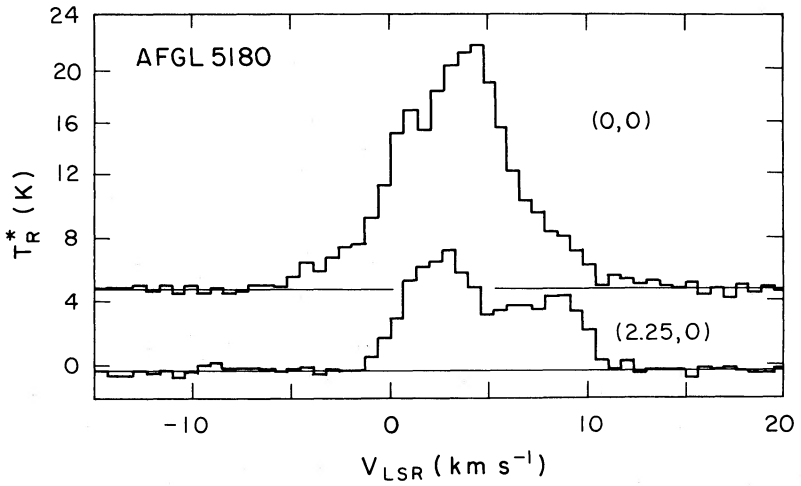

FIG. 11.—^{12}CO spectra obtained toward, and 2.'25 to the east of, AFGL 5180. The spectrum toward AFGL 5180 shows clearly the high-velocity red and blue wings, though the red wing may be contaminated by emission from a second velocity component at 9 km s^{-1} seen in the spectrum 2.'25 to the east.

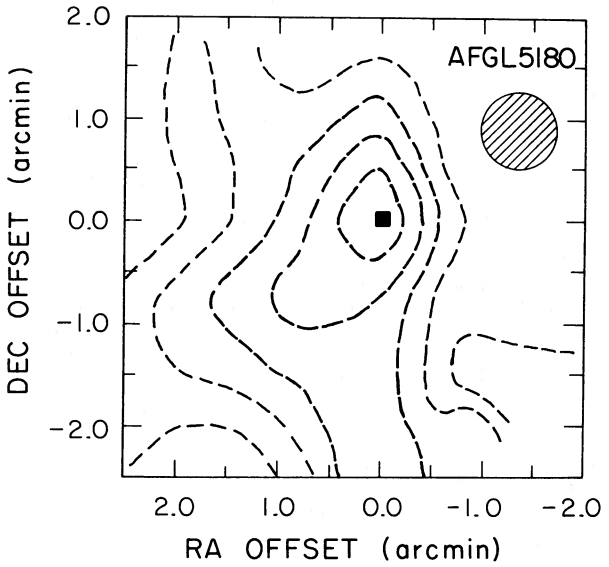

FIG. 12.—A map of the integrated ^{12}CO intensity of the high-velocity blueshifted (−8 to 0 km s^{-1}) emission near AFGL 5180. The redshifted emission is confused by a second velocity component at 9 km s^{-1}. The location of AFGL 5180 is indicated by a filled square and the FWHP beamsize is indicated by the cross-hatched circle.

velocity gas for the five outflows, integrated over the velocity intervals given earlier, are summarized in Table 3. To estimate the momentum and energy in the flows, we have computed the following integrals over the velocity range of the high-velocity redshifted and blueshifted gas:

$$\int T_R |(v - v_0)| \, dv$$

and

$$\int T_R (v - v_0)^2 \, dv \, ,$$

where v_0 is the velocity of the ambient cloud. The total momentum and energy in the outflows can be determined by converting to a column density and then summing the contributions to the momentum and energy from all parts of the map. Estimates of the momentum and energy contained in the outflows are presented in Table 3. Because the column density of high-velocity gas is only a lower limit and because no attempt was made to account for projection effects in estimating the velocity of the gas, the momentum and energy tabulated are also lower limits to their true values.

A comparison of the mass of high-velocity gas in these five outflows with that of other known outflows from young stellar objects of similar luminosity (Snell *et al.* 1984; Lada 1985; Snell 1987) shows them to be similar to the mean (though one has to remember that these are lower mass limits for the outflowing gas). However, a comparison of velocity indicates that the five flows have considerably smaller velocity extents than previously studied flows. In fact, the mass-weighted velocity for these outflows is only 3–6 km s^{-1}. Thus, it is not surprising that the momentum and energy of our outflows are also considerably less than those previously studied. Compared with outflow objects having similar mass and stellar luminosity, those studied here have 2–3 times less momentum and 10 times less energy.

The smaller velocities found for our sources as compared with previously studied regions may very well be a selection effect. The most obvious outflow sources, those with the most prominent line wings, were probably the first to be identified and only through more systematic surveys of young stellar objects, such as this one, are sources with less pronounced wings found.

We can estimate a dynamical time scale or "age" for our outflows by simply dividing their transverse sizes by their velocities. These estimates are presented in Table 3, and are conservative, in that we have used the smaller mass-weighted velocities, which are 2 to 3 times smaller than the maximum velocity observed. The average age is roughly 10^5 yr, considerably larger than the more energetic outflows studied by Snell *et al.* (1984). The difference in ages of our outflows with those previously studied may very well explain the corresponding difference in velocities, since one would expect outflow velocities to decrease with time as more and more material is accumulated in the outflowing molecular shell. One would also expect the mass of outflowing gas to increase with time, which does not seem to be the case. However, small outflow velocities make it difficult to distinguish accelerated gas from ambient molecular material, and thus, much of the outflowing material may be in fact missed. In addition, depending on the magnitude of the optical depth correction, the low-velocity outflows studied here may have substantially more mass. It therefore is reasonable to assume that age and velocity are inversely correlated and the outflows that we discovered are at the end of their detectable lifetime.

b) Statistics on Outflow Occurrence

We detected five outflows among the 18 young stellar objects that were included in our survey. Our search criteria also selected eight additional sources that we did not observe because they were already known to be outflow sources (Lada 1985). These are W3 OH, AFGL 437, AFGL 490, HH 12,

TABLE 3

PROPERTIES OF OUTFLOWS

Source	Mass ($M_\odot$)	Momentum ($M_\odot$ km s^{-1})	Energy (ergs)	Age (yr)	Mech. Luminosity ($L_\odot$)
AFGL 4029	9.7	33.1	1.2×10^{45}	1.7×10^5	0.06
AFGL 5142	4.9	14.3	6.0×10^{44}	2.0×10^5	0.03
AFGL 5157	7.6	37.1	2.0×10^{45}	1.9×10^5	0.09
AFGL 6366S.....	3.4	20.1	1.3×10^{45}	1.1×10^5	0.10
AFGL 5180[a]	2.3	12.7	7.6×10^{44}	6.8×10^4	0.09

[a] Properties of only the blue wing emission.

LkHα 101, S255 IRS1, AFGL 961, and NGC 2264. All eight of these would have been readily identified with our sensitivity and search strategy. Thus 13 of the 26 young stellar objects that met our selection criteria have molecular outflows associated with them. It is also interesting that the far-infrared luminosities of the previously known sources, with the exception of HH 12, lie in the range 2×10^3 to 1×10^5 $L_\odot$, similar to the range of far-infrared luminosities found for our sample. Thus, the 26 sources provide a relatively homogeneous sample of luminous, embedded, young stellar objects.

The selection of these 26 objects was not biased by prior information on molecular emission from these regions as has been the case in other surveys of luminous star-forming regions (e.g., Bally and Lada 1983). Therefore, the high detection rate of outflows must reflect a high incidence of the outflow phenomenon among luminous, young stars. Considering the possibility that outflows are often collimated and may lie in or near the plane of the sky, the incidence of outflows in these luminous objects is plausibly greater than 0.5.

c) *Implications on the Lifetimes of Far-Infrared Sources*

The high incidence of outflows among our sample sets a severe limit on the lifetime of objects as FIR sources. If FIR sources lived considerably longer than the detectable lifetime of outflows, one would expect to see many FIR sources without outflows, seen either before or after the duration of this event. Thus, based on the 50% detection rate the maximum lifetime of a FIR source is roughly twice the outflow lifetime. From our five newly detected outflows we can estimate that the detectable lifetime of outflows must be roughly 2×10^5 yr. Therefore, the material surrounding young O and B stars must be dispersed within 4×10^5 yr of first infrared light from these objects. Considering the possibility of a much higher incidence rate for outflows, it seems likely that cloud dispersal and the outflow phenomenon must go hand in hand and begin shortly after the young stars produce any substantial FIR luminosity.

It is difficult to assess the effect which our molecular outflows have on the surrounding molecular clouds, since we do not know the density or mass of the surrounding material. However, the time scales discussed above suggest that the outflows could play a major role in the dispersal of cloud material that surrounds the stars. The mass of the entire cloud can be estimated from our measured CO luminosity using the empirical relationship between luminosity and virial mass (Solomon *et al.* 1987). The masses of the clouds associated with the outflow sources are found to be typically 10^3–10^4 $M_\odot$. Clearly the momentum carried in a single outflow can have little effect on the stability of the entire molecular cloud.

However, the masses of the cloud cores in which these young stars formed contain considerably less mass; estimates for the masses of cores associated with compact H II regions are tens to hundreds of solar masses (Ho, Martin, and Barrett 1981). Although the cores may contain little of the total mass of the cloud, they generally provide most of the extinction to the young stellar objects. The momentum and energy estimated for the observed outflows are probably sufficient to disperse much of the core mass and to substantially reduce the visual extinction to the young stars. Hence, although one outflow may have little effect on the overall stability of its parent molecular cloud, continuous formation of O and B stars with winds may be responsible for maintaining the large turbulent motions observed in molecular clouds as well as for the eventual disruption of the entire cloud.

V. SUMMARY

The main points presented in this paper are the following.

1. Eighteen bright far-infrared sources with 100 μm flux densities greater than 500 Jy were surveyed for evidence of outflow activity in the $J = 1$–0 transition of CO. Five of the 18 sources have molecular outflows and three of these are clearly bipolar.

2. Molecular emission is associated with all 18 sources. This supports the argument that these sources are young stellar objects, as suggested by their infrared colors. The far-infrared luminosities of these objects indicate that they are all intrinsically luminous, massive young stars embedded in their parental material. They will most likely evolve into main-sequence O and B stars.

3. The detection rate of outflows from objects that satisfied our original selection criteria is 50%. This unbiased search suggests that the frequency of outflow activity associated with luminous young stars must be greater than 0.5.

4. The detection rate and outflow duration suggests that outflow activity must begin promptly after a source becomes a luminous far-infrared source. It also suggests that the lifetime of stars as bright far-infrared sources is only $\sim 4 \times 10^5$ yr, after which most of the surrounding material is dispersed and the visual extinction greatly reduced, probably by the action of the outflow activity.

The Five College Radio Astronomy Observatory is operated with support from the National Science Foundation under grant AST-85-12903 and with permission of the Metropolitan District Commission, Commonwealth of Massachusetts.

REFERENCES

Bally, J., and Lada, C. J. 1983, *Ap. J.*, **265**, 824.
Blitz, L., Fich, M., and Stark, A. A. 1982, *Ap. J. Suppl.*, **49**, 183.
Casoli, F., Dupraz, C., Gerin, M., Combes, F., and Boulanger, F. 1986, *Astr. Ap.*, **169**, 281.
Edwards, S., and Snell, R. L. 1984, *Ap. J.*, **281**, 237.
Emerson, J. P. 1987, in *IAU Symposium 115, Star Forming Regions*, ed. M. Peimbert and J. Jugaku (Dordrecht: Reidel), p. 19.
Evans, N. J., II, and Blair, G. N. 1981, *Ap. J.*, **249**, 394.
Evans, N. J., II, Blair, G. N., and Beckwith, S. 1977, *Ap. J.*, **217**, 448.
Georgelin, Y. M., and Georgelin, Y. P. 1976, *Astr. Ap.*, **49**, 57.
Georgelin, Y. M., Georgelin, Y. P., and Roux, S. 1973, *Astr. Ap.*, **25**, 337.
Goldsmith, P. F., Snell, R. L., Hemeon-Heyer, M., and Langer, W. D. 1984, *Ap. J.*, **286**, 599.
Heyer, M. H., Snell, R. L., Goldsmith, P. F., and Myers, P. C. 1987, *Ap. J.*, **321**, 370.
Ho, P. T. P., Martin, R. N., and Barrett, A. H. 1981, *Ap. J.*, **246**, 761.
Huang, Y.-L., and Thaddeus, P. 1986, *Ap. J.*, **309**, 804.
Humphreys, R. M. 1978, *Ap. J. Suppl.*, **38**, 309.
IRAS Point Source Catalog 1985, Joint *IRAS* Science Working (Washington, D.C.: U.S. Government Printing Office).
Kutner, M., and Ulich, B. L. 1981, *Ap. J.*, **250**, 341.
Lada, C. J. 1985, *Ann. Rev. Astr. Ap.*, **23**, 267.
Lada, C. J., and Wooden, D. 1979, *Ap. J.*, **232**, 158.
Levreault, R. M. 1985, Ph.D. thesis, University of Texas.
Loren, R. B., and Wootten, H. A. 1978, *Ap. J. (Letters)*, **225**, L81.
Moffat, A. F. J., FitzGerald, M. P., and Jackson, P. D. 1979, *Astr. Ap. Suppl.*, **38**, 197.
Price, S. D. 1977, *The AFGL Four Color Sky Survey: Supplemental Catalog.* Air Force Geophysics Laboratory, AFGL-TR-77-0160.
Price, S. D., and Walker, R. G. 1976, *The AFGL Four Color Sky Survey: Catalog of Observations at 4.2, 11.0, 19.8, and 27.4 μm*, Air Force Geophysics Laboratory, AFGL-TR-76-0208.
Roberts, W. W. 1972, *Ap. J.*, **173**, 259.
Sharpless, S. 1959, *Ap. J. Suppl.*, **6**, 257.

Snell, R. L. 1987, in *IAU Symposium 115, Star Forming Regions*, ed. M. Peimbert and J. Jagaku (Dordrecht: Reidel), p. 213.
Snell, R. L., Loren, R. B., and Plambeck, R. L. 1980, *Ap. J. (Letters)*, **239,** L17.
Snell, R. L., Scoville, N. Z., Sanders, D. B., and Erickson, N. R. 1984, *Ap. J.*, **284,** 176.
Solomon, P. M., Rivolo, A. R., Barrett, J., and Yahil, A. 1987, preprint.
Thronson, H. A., Schwartz, P. R., Smith, H. A., Lada, C. J., Glaccum, W., and Harper, D. A. 1984, *Ap. J.*, **284,** 597.
Wootten, A., Sargent, A., Knapp, G., and Huggins, P. J. 1983, *Ap. J.*, **269,** 147.

M. J. CLAUSSEN: Naval Research Lab., Code 4130, Washington, DC 20375

R. L. DICKMAN and R. L. SNELL: Five College Radio Astronomy Observatory, 619 Lederle Graduate Research Center, University of Massachusetts, Amherst, MA 01003

Y.-L. HUANG: Institute of History, Tsing-Hua University, Hsin-Chu, Taiwan, R.O.C.